Acta Biomaterialia 58 (2017) 365–375

Contents lists available at ScienceDirect

Acta Biomaterialia

journal homepage: www.elsevier.com/locate/actabiomat

Full length article

An interpenetrating, microstructurable and covalently attached conducting polymer hydrogel for neural interfaces

Carolin Kleber [a,b,*], Michael Bruns [c], Karen Lienkamp [b], Jürgen Rühe [a,b], Maria Asplund [a,b]

[a] BrainLinks-BrainTools Center, University of Freiburg, Germany
[b] Department of Microsystems Engineering (IMTEK), University of Freiburg, Germany
[c] Institute for Applied Materials (IAM) and Karlsruhe Nano Micro Facility (KNMF), Karlsruhe Institute of Technology, Karlsruhe, Germany

ARTICLE INFO

Article history:
Received 12 December 2016
Received in revised form 19 May 2017
Accepted 30 May 2017
Available online 31 May 2017

Keywords:
Neural interfaces
Conductive polymer hydrogel
Hydrogel
Conducting polymer
PEDOT
Surface modification
Electrodes
Drug delivery
Micropatterning
Surface attachment

ABSTRACT

This study presents a new conducting polymer hydrogel (CPH) system, consisting of the synthetic hydrogel P(DMAA-co-5%MABP-co-2,5%SSNa) and the conducting polymer (CP) poly(3,4-ethylenedioxythiophene) (PEDOT), intended as coating material for neural interfaces. The composite material can be covalently attached to the surface electrode, can be patterned by a photolithographic process to influence selected electrode sites only and forms an interpenetrating network. The hybrid material was characterized using cyclic voltammetry (CV), impedance spectroscopy (EIS) and X-ray photoelectron spectroscopy (XPS), which confirmed a homogeneous distribution of PEDOT throughout all CPH layers. The CPH exhibited a 2,5 times higher charge storage capacity (CSC) and a reduced impedance when compared to the bare hydrogel. Electrochemical stability was proven over at least 1000 redox cycles. Non-toxicity was confirmed using an elution toxicity test together with a neuroblastoma cell-line. The described material shows great promise for surface modification of neural probes making it possible to combine the beneficial properties of the hydrogel with the excellent electronic properties necessary for high quality neural microelectrodes.

Statement of Significance

Conductive polymer hydrogels have emerged as a promising new class of materials to functionalize electrode surfaces for enhanced neural interfaces and drug delivery. Common weaknesses of such systems are delamination from the connection surface, and the lack of suitable patterning methods for confining the gel to the selected electrode site. Various studies have reported on conductive polymer hydrogels addressing one of these challenges. In this study we present a new composite material which offers, for the first time, the unique combination of properties: it can be covalently attached to the substrate, forms an interpenetrating network, shows excellent electrical properties and can be patterned via UV-irradiation through a structured mask.

1. Introduction

Neural interfaces are gaining in importance as a methodology to treat, restore or investigate neurological dysfunctions based on both the recording of neural activity and the electrical stimulation of neuronal cells. Clinical applications include the treatment of paralysis, Parkinson's disease or the restoration of hearing with cochlear implants [1–4]. A major challenge to assure the long term functionality of such implantable devices consists in improving the integration of the implant into the neural tissue, for example by reducing the neuro-inflammatory response of the host. Persistent inflammation can lead to degradation or corrosion of the implant material, the loss of healthy neurons in the surrounding tissue, or the formation of an encapsulating layer – the glial scar. These mechanisms ultimately result in electrical insulation of the implant from the tissue and consequently a malfunctioning device [5–7]. To address this challenge, material-based strategies are urgently needed. Promising strategies involve the chemical modification of the implant surfaces using polymer coatings based on CPs or CPHs [5,8–11]. CP coatings such as PEDOT or polypyrrole (PPy) enhance the tissue-electrode communication by improving the electrical performance of the electrode. Furthermore, they have

* Corresponding author at: BrainLinks-BrainTools Center, University of Freiburg, Germany
E-mail address: carolin.kleber@imtek.uni-freiburg.de (C. Kleber).

http://dx.doi.org/10.1016/j.actbio.2017.05.056
1742-7061/

the potential to facilitate better tissue integration by immobilization of biomolecules on their surface or the release of drugs from their matrix through electrochemical switching [5,10,12,13]. Building on this idea, CPHs are material networks that consist of CPs grown within a hydrogel matrix. Hereby, the combination of both components opens up new possibilities to engineer smart and multifunctional materials. A wide range of CPH systems have been developed for applications in the field of neuroprosthetic devices [14–16], biosensors [17], drug-release devices [18–20] tissue engineering [21,22] and bioelectronics [23]. The hydrogel component provides a highly hydrophilic and porous network which can be filled with the CP in order to increase its electrical conductivity. The formation of a hybrid increases the storage volume accessible for the release of drugs and further facilitates the incorporation of biological components and cells into the electrode material [19,24]. As a result of its soft mechanical properties, it was proposed that the hydrogel can reduce the mechanical mismatch between the tissue and the electrode material and can act to stabilize the otherwise brittle CP [9,25]. The hydrogel itself can furthermore serve as an anti-biofouling surface preventing unwanted adhesion of proteins or inflammatory cells [26,27].

To successfully integrate CPHs as coating materials on neuroprosthetic devices, there are several design criteria that have to be met apart from the overall electrochemical performance and the biocompatibility of the material. Firstly, the CPH complex must be chemically and electrochemically stable, which is facilitated by a fairly homogenous integration of the CP into the hydrogel matrix. The deposition of a CP is typically performed by means of electrochemical polymerization, which requires the addition of an anionic dopant such as polystyrene sulfonate (PSS) or paratoluenesulfonate (pTS). Green et al. developed a strategy to achieve a true integration of the CP into the hydrogel by chemically attaching the anionic dopant to the hydrogel backbone [8]. The CP is then forced to grow along the hydrogel network forming a so called interpenetrating network (IPN).

Secondly, it is essential to ensure stable adhesion of the coating to the substrate electrode in order to avoid delamination of the CPH during the implantation procedure or during repeated CPH swelling and deswelling. The ideal way to achieve this is to establish covalent chemical bonds between the CPH and the substrate. A variety of different strategies have been developed to this end. For example, Guiseppi-Elie et al. have addressed this challenge by covalently attaching a poly(hydroxyethyl methacrylate) and PPy based CPH to a gold surface using a functionalization with 3-(aminopropyl) trimethoxysilane [28]. Prucker et al. have developed a different strategy by developing a procedure to covalently bind polymers to solid surfaces using benzophenone monolayers [29].

Thirdly, a critical part in making CPHs truly useful for microelectrode coatings is the opportunity to deposit and microstructure the material exclusively at selected sites on the probe. Commonly used electrodes for neural applications can have diameters as small as 20–150 μm [30–32]. Consequently, it is of great importance to establish a fabrication process which allows the patterning of CPHs within this size range. A study reported by Pan et al. showed the micropatterning of a phytic acid gelated and doped polyaniline hydrogel using ink-jet printing or spray coating methods [23]. Although CPHs meeting the single design criteria have been presented in previous studies, a CPH system offering a combination of the listed requirements has, to our knowledge, not been reported yet.

In this work, we present a CPH, which can be patterned with a photolithographic process, forms an IPN and can be covalently attached to the substrate electrode via ultraviolet light (UV)-reactive 4-(3-triethoxysilyl)propoxybenzophenone (3-EBP) silane. The CPH is composed of the synthetic hydrogel P(DMAA-co-5% MABP-co-2,5%SSNa) (PDMAAp) and the CP PEDOT (Fig. 1). The

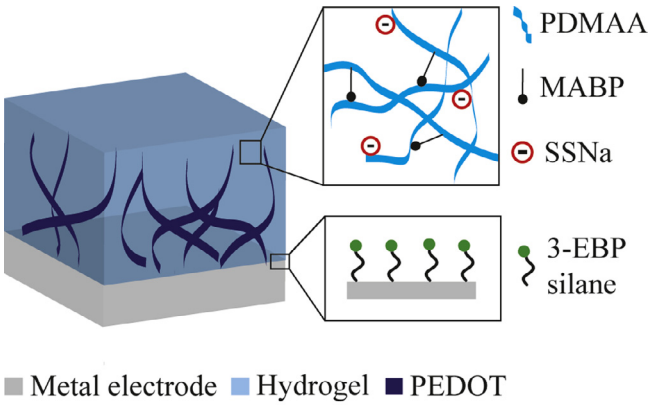

Fig. 1. Schematic depiction of the CPH composition. The hydrogel component PDMAAp consists of the PDMAA backbone, the MABP crosslinker and the SSNa units, which serve as counterions during the deposition of PEDOT. The hydrogel is covalently attached to the surface with 3-EBP silane.

hydrogel component is a copolymer consisting of dimethylacrylamide (DMAA), sodium 4-styrenesulfonate (SSNa), which serves as the anion for the deposition of PEDOT, and the UV-reactive 4-methacryloyloxy benzophenone (MABP). Hydrogels based on PDMAA have already been investigated for several biomedical applications and have shown to serve as protein-repellent coating materials [27,33–36]. In general, a synthetic hydrogel offers high control and reproducibility of its chemical composition, mechanical properties, microstructure, and degradation rate. It can be produced at low costs and is at low risk for immune responses since it does not contain biological impurities [37,38]. This indeed holds true also for the PDMAAp which, for example, can be tuned with respect to its chemical, mechanical and electrochemical characteristics and be modified with bioactive agents [33]. The choice to use PEDOT as CP component is based on its superior electrochemical stability in comparison to PPy [39]. In this work, the CPH was characterized using CV, EIS, XPS and water contact angle measurements. In addition, non-toxicity was verified using an elution toxicity test with a neuroblastoma cell line.

2. Materials and methods

2.1. Sample fabrication

Two types of test samples were designed and fabricated for this work. The first type, as illustrated in Fig. 2a was used for the electrochemical characterization and the XPS analysis. Each sample consists of a single electrode site (2,0 mm in diameter) realized on a Pyrex substrate (0,5 × 5,0 × 30,0 mm). The image reversal resist AZ 5214E (Microchemicals GmbH, Ulm, Germany) was used to form the tracks for the deposition of the metal layers. Sputter deposition with a Leybold Univex 500 sputter device (Oerlikon Leybold Vacuum GmbH, Germany) was applied to deposit a layer of titanium (Ti, 50 nm), platinum (Pt, 150 nm) and iridium oxide (IrO_x, 800 nm). The IrO_x layer was deposited selectively onto the electrode site and the interconnection line by reactively sputtering iridium in an oxygen plasma. The metals were patterned with a lift-off process. The samples were insulated with a 30 μm thick negative photoresist (SU-8 3025, MicroChem. Corp., USA). The relatively large electrode dimensions of this test sample were chosen to facilitate the exploration and development of the CPH.

The second type of test samples, as illustrated in Fig. 2b, served as a test platform for the cell culture study and the water contact angle measurements. For these experiments, a large electrode area was required to obtain a high ratio of exposed electrode material to

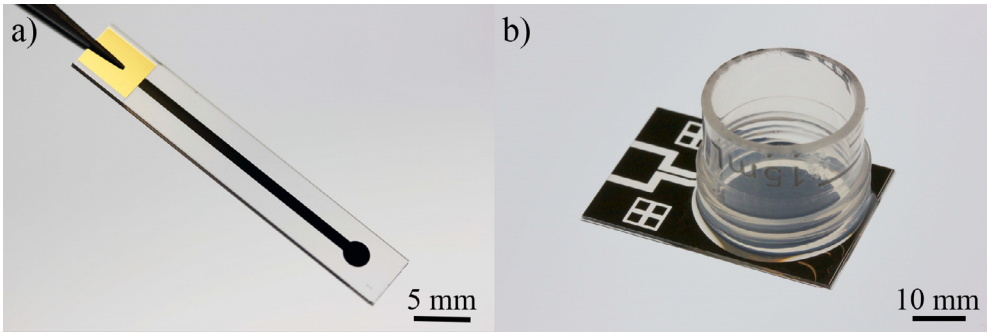

Fig. 2. Photographic images of test samples used for the electrochemical analysis and the XPS measurement (a) and the cell culture and water contact angle measurements (b).

cell culture volume. The final sample consisted of a single IrO_x electrode site with a diameter of 13,59 mm. The metals, Ti/Pt/IrO_x (50 nm, 150 nm, 800 nm) were sputter deposited on a glass wafer and microstructured with a laser (DPL genesis Marker, ACI Laser GmbH, Germany). Cell culture wells were realized by mounting cell vials (Falcon tube, VWR, Germany) on top of each electrode using a two component silicone (Sylgard 184, Dow Corning, USA).

In addition, glass substrates were sputter coated with indium tin oxide (ITO, 100 nm in thickness) using the Univex 300 sputter device (Oerlikon Leybold Vacuum GmbH, Germany). The transparent ITO substrates were used to evaluate the color change resulting from the deposition of PEDOT throughout the hydrogel matrix.

2.2. Preparation of polymer coatings

For all electrochemical measurements in this work, a potentiostat (PGSTAT 102 N, Metrohm Autolab, Germany) was used in a conventional three-electrode setup. The IrO_x electrode served as the working electrode, a stainless steel sheet as the counter electrode and a silver/silver chloride (Ag/AgCl) electrode (BASI, USA) as the reference. Prior to usage, the microfabricated probes were cleaned in acetone, isopropanol and deionized water. The IrO_x electrodes were electrochemically activated by CV in 0,01 M phosphate buffered saline solution (PBS, Sigma Aldrich, Germany) for 300 cycles at sweep rate of 0,2 V/s between the potential limits of −0,6 and 0,8 V. An overview of the CPH fabrication process is provided in Fig. 3.

2.2.1. Functionalization with 3-EBP silane

To enable covalent binding between the hydrogel and the substrate, the IrO_x electrodes were chemically functionalized with the crosslinking agent 3-EBP silane, which was synthesised according to procedures given in literature [40]. The functionalization of the IrO_x electrodes was performed by spin coating a solution of 3-EBP silane (20 mg ml^{-1} in toluene) onto the microfabricated probes (3000 rpm for 30 s). The samples were cured on a preheated hot plate at 120° for 30 min, washed with toluene and dried under a flow of nitrogen. Samples were stored in the dark at room temperature.

2.2.2. Hydrogel synthesis, coating and crosslinking

The polymer PDMAAp was prepared by radical polymerization according to procedures described elsewhere [41]. The obtained hydrogel precursor (30 mg/ml in 99% ethanol) was deposited onto the 3-EBP silane pretreated samples using a dip coating procedure (ND-R Rotary Dip Coater, Nadetech Innovations, Spain). It was cross-linked and patterned by UV exposure with a total dosage of 2 J cm^{-2} at 365 nm (Bio-Link 365, Vilber Lourmat, Germany) through a laser structured MP35N foil mask (Hamilton Precision

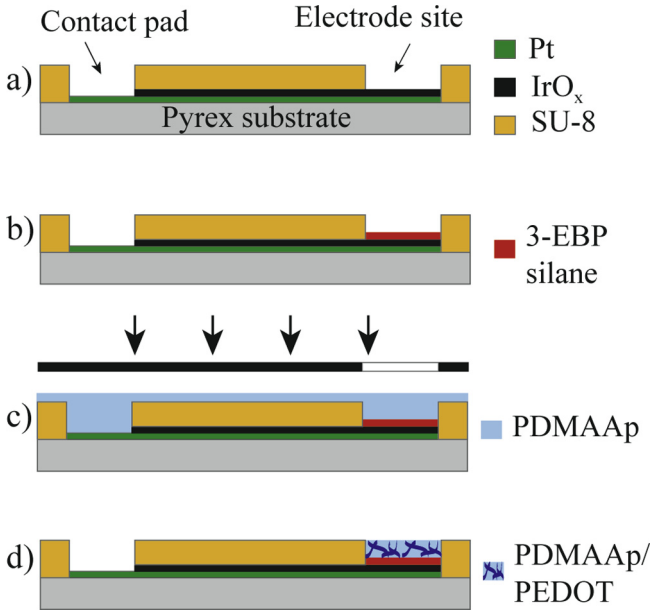

Fig. 3. Schematic of the CPH fabrication process. The test sample (a) is functionalized using 3-EBP silane (b) and coated with hydrogel using a dip coating procedure. Hydrogel crosslinking is performed by UV-illumination at 365 nm through a patterned mask to achieve hydrogel structures on top of the selected electrode site (c). PEDOT is electrochemically deposited throughout the hydrogel network (d).

Metals, USA). The samples were then washed with 99% ethanol to extract unreacted polymer chains. The thickness of the hydrogel was controlled by the number of dips and the concentration of the hydrogel precursor. A hydrogel of an approximate thickness of 1,2 μm in the dry state was obtained by building up three hydrogel layers, which were formed by repeating the previously described coating and crosslinking procedure. This thickness was selected as a starting point to demonstrate the feasibility of this layer by layer deposition. Depending on the application, thickness can easily be varied for future applications by controlling the number of layers included.

Additional experiments were performed to explore the possibility of the CPH to be patterned to smaller dimensions and different geometries. IrO_x substrates were functionalized with 3-EBP silane and coated with a single hydrogel layer. This layer was crosslinked with UV-light (2 J cm^{-2} at 365 nm, Newport Oriel Instruments, USA) through a foil mask. The smallest tested structures consisted of round circles (100 μm in diameter) and line structures (20 μm in width).

2.2.3. PEDOT/PSS polymerization

3,4-Ethylendioxythiophene (483028, EDOT < 97%) was obtained from Sigma Aldrich. Prior to deposition, the hydrogel coated samples were soaked in EDOT solution for approximately 1 h to allow swelling of the gel and equilibration of the EDOT monomer throughout the hydrogel. PEDOT/PSS was polymerized through the hydrogel mesh by galvanic deposition from an aqueous solution containing 0,01 M EDOT at a current density of 0,125 mA/cm^2 and a charge cut-off of 0,17 mC/cm^2 for both sample types. These parameters were found to be high enough to enable the deposition of PEDOT, but low enough to avoid over-oxidation of the material. No additional supporting electrolyte was required since the counterion PSS was supplied by the hydrogel. The finished samples were washed in deionized water to extract unreacted EDOT, dried under a flow of nitrogen and stored in the dark at room temperature. PEDOT/PSS reference samples were prepared by galvanic deposition onto plain IrO_x electrodes from an aqueous solution containing 0,01 M EDOT and 71 μM PSSNa (Sigma Aldrich) at a current density of 0,125 mA/cm^2 and a charge cut-off of 0,17 mC/cm^2 for both sample types. To facilitate the comparison between the CPH and PEDOT/PSS samples, identical deposition parameters were chosen.

2.3. Electrochemical characterisation

The electrochemical analysis was performed by means of CV and EIS. A potentiostat (PGSTAT 102N, Metrohm Autolab, Germany) was used in a conventional three-electrode setup as described previously. The experiments were carried out in a 0,01 M PBS solution. Prior to the measurements, the hydrogel coated samples were immersed in PBS for approximately 1 h to ensure swelling and homogeneous distribution of ions throughout the gel. CV (n = 1000) was applied over the sweep range of −0,6 V and 0,8 V (vs. Ag/AgCl) at a scan rate of 0,1 V/s. The CSC for each scan was calculated as the charge enclosed within one CV cycle using the software Origin Pro 2017 (OriginLab, USA). EIS was performed over the range of 0,1 Hz to 10 kHz using a sinusoidal excitation signal with an amplitude of 10 mV. For each material, the −3 dB cut-off frequency was determined at the −45° phase shift angle and was used as a quality measure of film conductivity.

Additional experiments were conducted to evaluate the long-term performance of the CPH material when immersed in PBS or standard cell culture medium over 10 days. For this study, CPH coated samples were sterilized in 70% ethanol overnight and washed with sterilized water (Sigma Aldrich). The samples were then immersed in sterilized PBS (0,01 M) or standard cell culture medium (as described in Section 2.6) and placed in an incubator at 37 °C and 5% CO_2 for 10 days. CV and EIS measurements were performed after 0,5 h/6 h/1 day/2 days/4 days/7 days and 10 days after first immersion. After every measurement, the samples were washed with deionized water and placed in new PBS or cell culture medium.

2.4. X-ray photoelectron spectroscopy

XPS measurements were performed using a K-Alpha+ XPS spectrometer (Thermo Fisher Scientific, East Grinstead, UK). Data acquisition and processing using the Thermo Avantage Software is described elsewhere [42]. All samples were analyzed using a microfocused, monochromated Al Kα X-ray source (30–400 μm spotsize). The K-Alpha charge compensation system was employed during analysis, using electrons of 8 eV energy and low-energy argon ions to prevent any localized charge built-up. The spectra were fitted with one or more Voigt profiles (binding energy uncertainty: ±0,2 eV). The analyser transmission function, Scofield sensitivity factors [43], and effective attenuation lengths (EALs) for photoelectrons were applied for quantification. EALs were calculated using standard TPP-2M formalism [44]. All spectra were referenced to the C1s peak of hydrocarbon at 285,0 eV binding energy controlled by means of the well-known photoelectron peaks of metallic Cu, Ag and Au. Sputter depth profiles were performed using a raster scanned Ar^+_{1000} cluster ion beam at 8,0 keV, 30° angle of incidence and a sputtered area of 2 × 4 mm^2.

2.5. Contact angle measurement

Static as well as advancing and receding contact angles were assessed with an OCA 20 device (Dataphysics GmbH, Filderstadt, Germany) using deionized and filtered Millipore water (drop size ≈ 5 μl). Contact angles were calculated using an elliptical or tangential fitting method. All measurements were obtained from three samples each measured at three different points.

2.6. Cell culture

A cell elution test, as described in ISO 10993-5, was performed to verify non-toxicity of the CPH. The human neuroblastoma cell line SH-SY5Y was obtained from the European Collection of Authenticated Cell Cultures (ECACC). The cells were maintained at 37 °C and 5% CO_2 in Dulbecco's Modified-Eagle's Medium (DMEM with 2 mM Glutamine, Sigma Aldrich) and supplemented with 15% Fetal Bovine Serum (FBS, Sigma Aldrich), 1% Non-essential amino acid solution (M7145, Sigma Aldrich) and 1% Penicillin-Streptomycin (Sigma P4333). Prior to medium exposure, all samples were sterilized in 70% ethanol overnight and washed with sterilized water (Sigma Aldrich). The extracts were prepared by exposing the test material to the standard cell culture medium at three different concentrations (1,25 cm^2/ml, 2,0 cm^2/ml, 2,75 cm^2/ml) for 24 h at 37 °C. The SH-SY5Y cells were cultured for 24 h in a 96 well plate (1,8 × 10^3 cells/well). Each well was then exposed to 100 μl of test extract of one concentration. For each material and concentration a total number of 10 wells were prepared, except for the IrOx sample at a concentration of 2,75 cm^2/ml (n = 9). Cells grown in the standard cell culture medium served as a negative control. For the positive control, the cells were treated with the toxic Triton-X-100 (Sigma Aldrich). The cell viability was assessed after 26 h of incubation using a standard 3-(4,5-dimethylthiazolyl-2)-2,5-diphenyl-tetrazolium bromide (MTT, Sigma Aldrich) colorimetric assay [45]. Hereby, the MTT salt was added to each well which was further incubated for 4 h. After the incubation, cells in each well were treated with 50 μl dimethylsulfoxide (DMSO, Roth) and incubated for 10 min. The absorbance was measured at 595 nm using an Elisa plate reader (Enspire, Perkin Elmer GmbH, Rodgau, Germany). The average viability was calculated as percentage of the negative control, which was determined to represent 100 % viability.

2.7. Statistical analysis

Data was tested for normality and equal variances using the Anderson-Darling test and the Levene's test. Statistical comparison of static water contact angles as well as the CSCs and cut-off frequencies between the different materials at cycle 10 was performed using a one-way ANOVA followed by a Welch's *t*-test. To evaluate differences in CSC before and after repetitive cycling as well as after the longevity study in PBS or cell culture medium, the non-parametric Wilcoxon signed rank test was used. In vitro data was analyzed with a two-way ANOVA and a Tukey test. One outlier within the dataset of the positive control at a concentration of 2,75 cm^2/ml was identified and removed using the Grubb's test. If not stated otherwise, the data is expressed as mean ± standard deviation (SD). Significance was determined with $p < 0.05$.

Table 1
Water contact angles measured for IrO_x and 3-EBP treated substrates (n = 9).

	IrO_x	Silane anchor
Static WCA [°]	56,3 ± 6,2	111,0 ± 3,1
Advancing WCA [°]	74,0 ± 5,6	114,4 ± 4,5
Receeding WCA [°]	0,0 ± 0,0	4,4 ± 4,8

Statistical analysis was performed with the software Origin Pro 2017 (OriginLab, USA).

3. Results

3.1. Preparation of CPH coatings

In this work, we developed a CPH coating which consists of the hydrogel PDMAAp and the CP PEDOT. A schematic of the individual CPH components is given in Fig. 1. Covalent attachment of the CPH onto the substrate electrodes was realized via 3-EBP silane anchors as described elsewhere [46]. The functionalization of IrO_x surfaces has, however, not been demonstrated in literature until now. Water contact angle measurements confirmed the successful immobilisation of 3-EBP silane onto IrO_x substrates. As shown in Table 1, static water contact angles increased significantly by 54,7° from the untreated IrO_x substrates (56,3° ± 6,2) to the 3-EBP treated ones (111,0° ± 3,1) and indicate the presence of the hydrophobic benzophenone groups on the IrO_x surface. The hydrogel was deposited onto the functionalized substrates with a dip coating procedure. Crosslinking and surface attachment was achieved via UV-irradiation through a patterned mask. Hereby, only the hydrogel parts exposed to UV-light were crosslinked and attached to the selected electrode site. Unreacted polymer chains were washed away by immersion in ethanol for at least 1 h.

In order to demonstrate the feasibility of this photolithographic technique to generate hydrogel structures in the microscale, we performed patterning experiments with geometries and dimensions ranging from 20 to 150 μm. Due to resolution limitations of the foil mask, smaller dimensions were not tested.

Fig. 4 shows micrographs of a patterned hydrogel layer on functionalized IrO_x substrates. The images display typical structures as found on microfabricated neural probes: Arrays of microdots (100 μm in diameter, Fig. 4a), tracks with different widths (20–40 μm, Fig. 4b) or rectangles as used for alignment markers (140 μm, Fig. 4c). We could demonstrate the successful patterning of the hydrogel into structures as small as 20 μm. As shown in Fig. 4d, the obtained edges appear slightly irregular at higher magnification. This is expected since foil masks were used, which are likely to have limited edge precision. We expect that smaller resolutions and greater precision can be reached when using a mask-aligner system together with a chrome mask at cleanroom conditions.

PEDOT was successfully integrated into the already patterned hydrogel matrix through a combination of electropolymerization and establishment of ionic interactions between the negative charges of the sulfonate in the hydrogel and the positive charges on the PEDOT. As a result, the final CPH is automatically patterned since the PEDOT can only grow where the hydrogel is situated. When transparent ITO substrates were used, this deposition resulted in a color change of the previously colorless hydrogel to a blue color. Since the IrO_x surface is dark, it was difficult to clearly assess this color change on this material visually.

3.2. Electrochemical characterization

The electrochemical performance of CPHs in comparison to IrO_x, the unmodified PDMAAp hydrogel and PEDOT/PSS samples was evaluated using EIS and CV. The CSC, obtained from the area enclosed by one CV cycle, was used as a measure to allow comparison between the different materials. Fig. 5a shows a clear increase of the average CSC of the hydrogel (10,6 ± 0,2 mC/cm^2) when

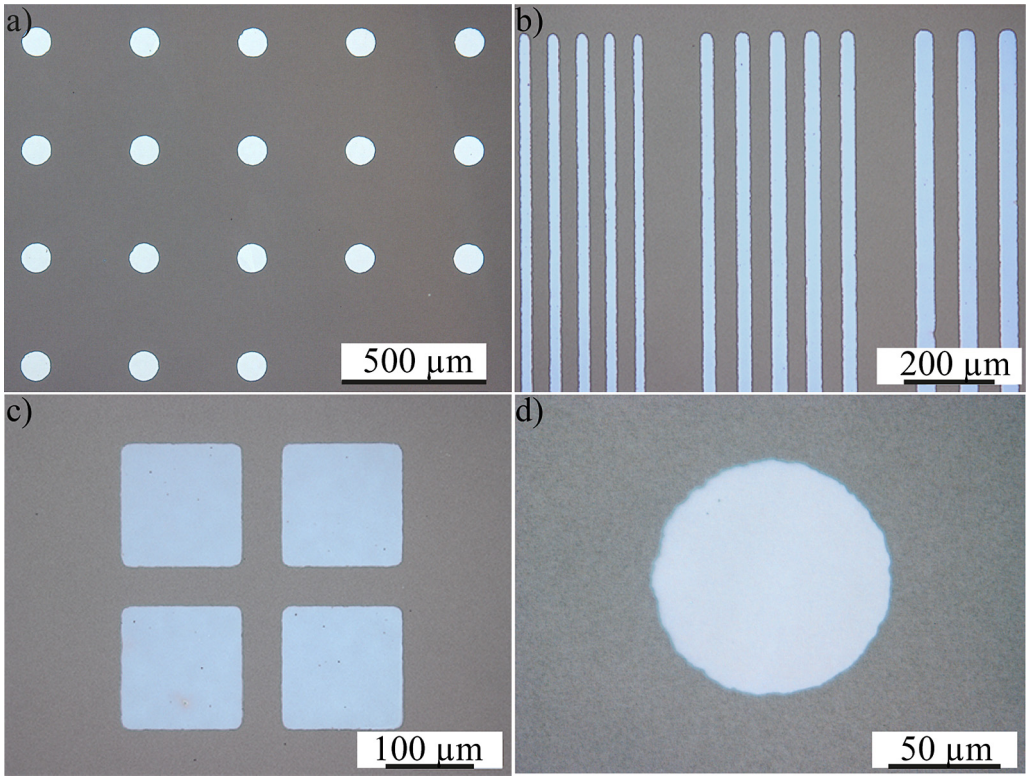

Fig. 4. Microscopic images of micropatterned hydrogel structures. IrO_x substrates were coated with a single layer of hydrogel, crosslinked and patterned though a foil mask using UV-light (2 J cm^2 at 365 nm, Newport Oriel Instruments, USA).

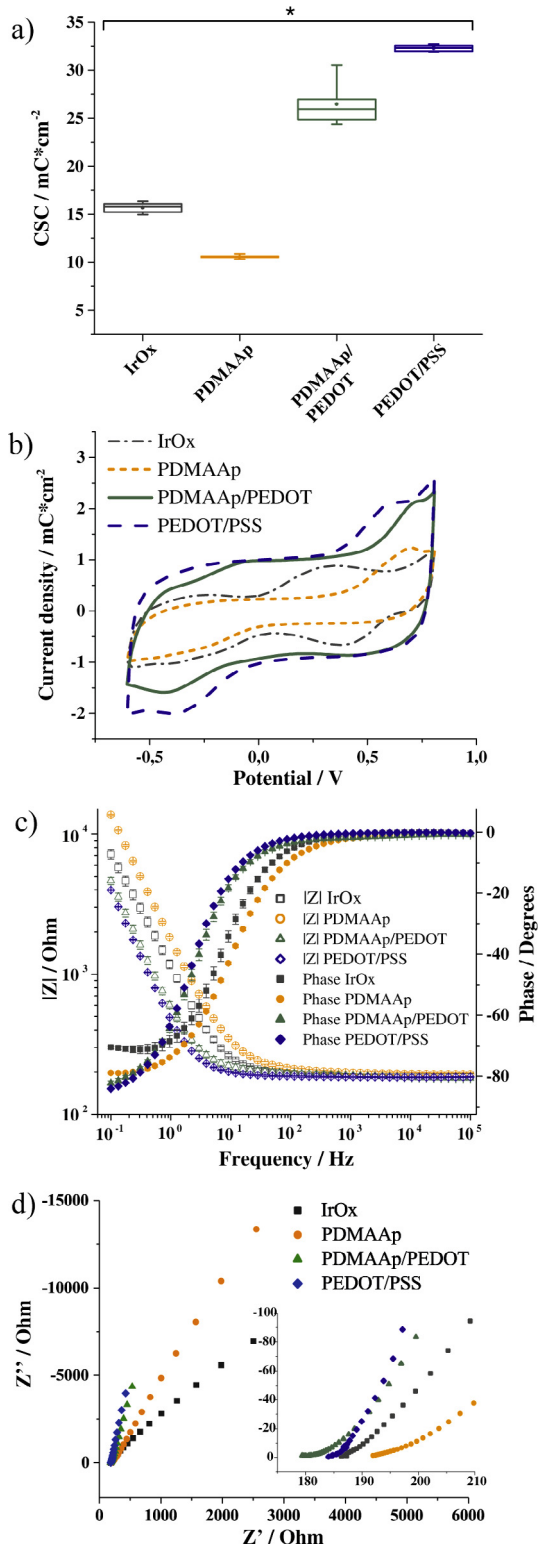

Fig. 5. Electrochemical characterization of CPH, IrO_x, the unmodified PDMAAp hydrogel and PEDOT/PSS samples. Box plots (n = 6) show the CSCs obtained from the area enclosed of a CV sweep at cycle 10. The whiskers represent the minimum and maximum values. Mean values are represented with dots. The data shows a significant increase in CSC as a result of the PEDOT deposition throughout the hydrogel matrix. ($^*p < 0.05$) (a). Exemplary CV curves at cycle 10 for each material (b). The mean impedance and phase over the frequency range of 0,1 Hz–10 kHz at cycle 10 (c). Error bars represent one SD (n = 6). PEDOT incorporation into the hydrogel results in a significantly decreased cut-off frequency ($p < 0.05$). The Nyquist plot shows exemplary results of the EIS measurements for each material (d).

extended into a CPH (26,5 ± 2,2 mC/cm^2) indicating that successful deposition of PEDOT took place throughout the hydrogel matrix. Statistical analysis using a one-way ANOVA and a Welch's *t*-test confirmed the statistical significance of this 2,5-fold increase ($p < 0.05$). Exemplary CVs performed at cycle 10 for each material are given in Fig. 5b. The addition of PEDOT into the hydrogel leads, as expected, to an enlarged area comparable to that of the PEDOT/PSS control. The impedance analysis as shown in the Bode diagram and the Nyquist plot (Fig. 5c, d) supports that PEDOT was successfully integrated within the hydrogel to form a hybrid material. The impedance of the CPH is reduced by one order of magnitude in the lower frequency range < 10 Hz when compared to the bare hydrogel. The cut-off frequency of the CPH (3,1 ± 0,2 Hz) is significantly smaller than the one obtained for both the bare hydrogel (11,9 ± 0,6 Hz) and the IrO_x samples (9,3 ± 0,9 Hz). In addition, no significant difference was found between the cut-off frequency of the CPH and the PEDOT/PSS (2,5 ± 0,1 Hz). The electrochemical stability and long-term performance of the CPH system was investigated by extensive CV cycling in PBS as well as the immersion of the CPH samples in PBS or cell culture medium for 10 days at 37 °C and 5 % CO_2 (Fig. 6). After repetitive CV cycling with 1000 CV sweeps, the CSC of the CPH decreased by 1,9% when comparing the CSC at cycle 10 and 1000. No significant difference could be confirmed using the Wilcoxon signed rank test. In comparison, the PEDOT/PSS shows a significant loss of 5,5%, while the average CSC obtained for the bare hydrogel and IrO_x samples increase by 36,4% (significant) and 6,0% (not significant) (Fig. 6a). To demonstrate the origin in variability for the CPH samples, the individually measured CSCs for each of the six CPH samples are shown in Fig. 6b. Despite one exception, the individual data points are situated within a similar CSC range which proves that the large variability can be attributed to the one outlier in an otherwise consistent dataset. In addition to the repetitive cycling, the CPH were immersed in PBS or cell culture medium under physiological conditions for 10 days. Comparison of the CSC at 0,5 h and 240 h after first immersion in PBS and cell culture medium revealed a significant increase in CSC of 5,7% and 3,0% respectively (Fig. 6c). This increase is likely the result of activation and hydration processes happening within the CPH, which make the material even more conductive. The impedance data, as given in the Nyquist plot, show similar curve shapes at 0,5 h and 240 h for both the PBS and the cell culture medium, which speak for the electrochemical stability of the CPH system (Fig. 6d). No sign of delamination of the CPH was found neither over the 1000 CV cycles nor during the long-term immersion in PBS or cell culture medium.

3.3. X-ray photoelectron spectroscopy

XPS analysis was performed to examine the composition of the CPHs and to confirm the presence of PEDOT within the hydrogel matrix. In particular, Ar^+_{1000} cluster ions were used for sputter depth profiling to preserve the chemical information during the removal of the organic material. However, the used cluster ion beam cannot sputter etch the IrO_x layer and, therefore, the profile is interrupted when approaching the interface as depicted in Fig. 7c. The differentiation between the unmodified PDMAAp hydrogel and the CPH was assessed with S 2p spectra. The obtained S 2p spectra for the hydrogel and the CPH samples are provided in Fig. 7a. In good agreement with literature, the S $2p_{3/2}$ peak of the C—S groups stemming from the PEDOT are found at 163,7 eV binding energy whereas the C—SO_3— group solely present in the hydrogel (PSS) appears at S $2p_{3/2}$ = 167,5 eV [47,48]. Additionally to the C—SO_3—, the hydrogel contains a N—C=O group found at N 1s = 400,0 eV (not shown here), which directly can serve as a second marker for the hydrogel [49]. The S 2p spectra taken from the

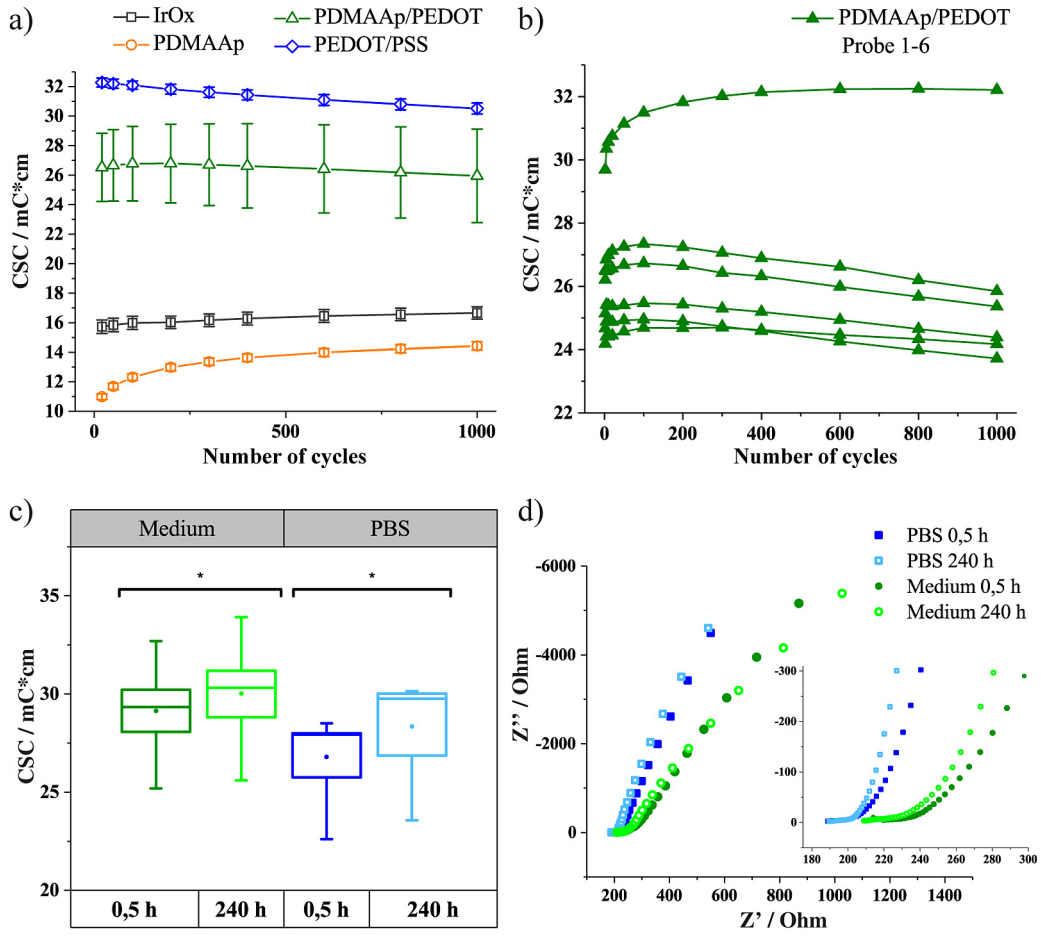

Fig. 6. Electrochemical stability analysis of CPH samples and control groups. The mean CSC of the different materials is shown vs. repetitive cycling (n = 1000 cycles) in PBS. Error bars represent one standard deviation (n = 6). No significant change was found when comparing the CSC of the CPH samples at cycle 10 and 1000 ($p < 0.05$). The data shows the individually measured CSC for the CPH samples over the 1000 CV sweeps (b). The box plots display the CSC of CPH samples immersed in PBS or cell culture medium after 0,5 h and 10 days. The whiskers represent the minimum and maximum values. Mean values are represented with dots. The CSC increase significantly when comparing the CSC at 0,5 h and 10 days ($^{*}p < 0.05$). Exemplary results from the EIS measurements of the CPH samples after 0,5 h and 10 days of immersion in PBS or cell culture medium are given in the Nyquist plots (d).

different levels of the performed sputter depth profiles prove that no sputter induced degradation has to be considered and, moreover, they directly evidence the homogeneous infiltration of PEDOT within the hydrogel matrix across the complete layer thickness. Note that for a better visualisation, the spectra are normalized to maximum intensity, and, therefore, quantitative information is only available from the respective sputter depth profiles shown in Fig. 7b for a pure hydrogel layer and in Fig. 7c for the infiltrated PDMAAp/PEDOT system. The profiles shown here comprise only the most relevant groups and the profiles of the complete elemental inventory are depicted in the Supplemental information (Fig. S1). A comparison of both sputter depth profiles clearly evidences the homogeneous distribution of PEDOT (C—S group) within the hydrogel (C—SO_3— and N—C=O groups) and additionally demonstrate that there is no substantial chemical change of the hydrogel as a result of the deposition of PEDOT.

3.4. Cell culture

An elution toxicity test was performed with the neuroblastoma cell line SH-SY5Y to verify non-toxicity of the CPH material. The cells were exposed to material extracts at three different concentrations of 1,25 cm^2/ml, 2,0 cm^2/ml and 2,75 cm^2/ml for 26 h at 37 °C. Different concentrations were tested since the cell viability should be independent of extract concentration for non-toxic materials. Fig. 8 shows boxplots with the average absorbance at 595 nm measured for each material and extract concentration. The absorbance acquired for cells exposed to CPH is situated in the same range as the negative control at all test concentrations. Statistical analysis using a two-way ANOVA model demonstrated that there was no significant difference between these two data sets. As expected, the difference between the absorbance acquired for the CPH and the positive control are significantly different. Since the absorbance values of the negative control can be associated with 100 % cell viability, the mean viability for each test materials was calculated. In fact, the cells exposed to CPH extracts exhibit an average viability of 106%, 98% and 85% at the concentrations of 1,25cm^2/ml, 2,0cm^2/ml and 2,75 cm^2/ml respectively. This high viability at all concentrations supports the non-toxicity of the hybrid CPH materials. Furthermore, the cells were healthy, adherent and showed no morphological difference when compared to the negative control under a microscope. A decreased viability was calculated for all material extracts at the concentration of 2,75 cm^2/ml. At this concentration, however, the absorbance measured for the negative control, which serves as the reference point, was much higher when compared to the other concentrations, indicating that the calculated decrease in viability is due to an increased reference point.

4. Discussion

The aim of this work was to develop a novel CPH which can serve as coating material for neural interfaces combining the beneficial properties of a hydrogel with the excellent electronic properties provided by PEDOT. For such a coating it is not only important to meet the electrochemical requirements for the recording and stimulation to and from neural tissue, but also to consider design criteria which ensure a stable and homogeneous coating, that is covalently attached to the substrate electrode and can be patterned onto selected electrode sites. To realize this goal, we developed a hybrid between the highly tuneable synthetic hydrogel P(DMAA-co-5%MABP-co-2,5%SSNa) and the CP PEDOT. The first design criterion for developing a stable and homogenous coating was accomplished by forming an IPN between the hydrogel and the PEDOT component. The anionic dopant PSS, which is needed for the deposition of PEDOT, was chemically linked to the hydrogel network. Since the deposition was performed from an EDOT solution without supporting electrolyte, any growth of the PEDOT chains leads to a permanent integration into the hydrogel scaffold. Since PEDOT is bound to the immobile dopants through ionic interactions and not covalently cross-linked, we suggest that this network is semi-interpenetrating (sIPN). Interpenetration of the hydrogel matrix implies that the CP is equally distributed throughout the material. If the distribution of the CP is inhomogeneous, for example if predominantly deposited near the metallic electrode surface, the hydrogel would act as an insulator and the distance between the neurons and the electrically active surface would be increased [50]. The formation of a sIPN/IPN thereby ensures that the CPH acts as one functional unit, which is important for its mechanical and electrochemical stability.

We were able to confirm homogeneous distribution of PEDOT within the hydrogel matrix by XPS analysis and further confirm its presence by EIS and CV. As XPS can identify the different oxidation states of the sulfur groups associated to PEDOT or PSS within the hydrogel, the S 2p peak was used to distinguish between the both components of the CPH, corroborated by the N 1s signal stemming only from the hydrogel [49].

We obtained a significant increase by 2,5-fold in CSC as well as a reduction in impedance and cut-off frequency as a result of the PEDOT deposition. These values are similar to what is obtained for the PEDOT/PSS films which is a strong indication for that PEDOT integration was truly successful. The presented values for the CSC were here used as a quality measure to compare the materials analyzed within this study and describe the amount of charge transfer taking place in response to a slow sweep over oxidising and reducing potentials.

Goding et al. examined the role of dopant density and interdopant spacing for the deposition of PEDOT throughout a hydrogel matrix. They could demonstrate that smaller interdopant spacing results in increased electroactivity of the CPH system suggesting a larger presence of PEDOT within the hydrogel matrix [50]. Since the current composition of the hydrogel contains only 2,5% of the immobile dopant SSNa, we suggest that the incorporation of a higher percentage of SSNa within the hydrogel might result in a higher amount of PEDOT infiltration making the coating even more conductive.

CVs were furthermore used as a method do evaluate surface adhesion and mechanical stability of PEDOT based coating materials as previously described by Boehler et al. [51]. As a result of oxidation and reduction, CPHs will experience mechanical stress due to the expansion and contraction driven by ionic exchanges. For

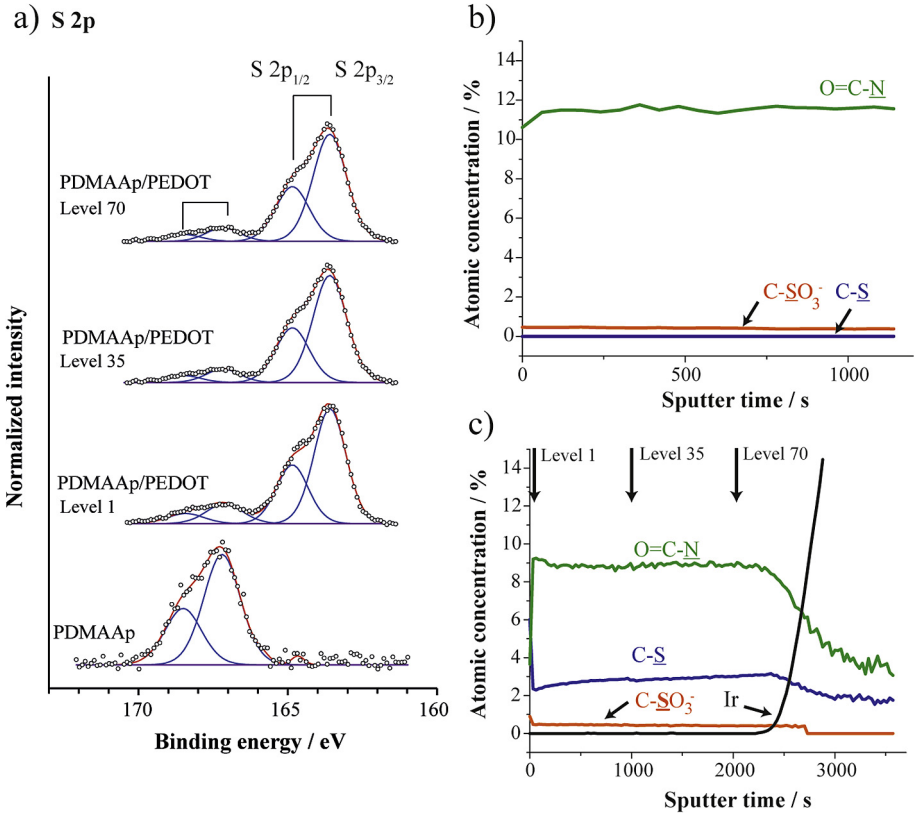

Fig. 7. XPS characterization of the CPH and the unmodified PDMAAp hydrogel. The S 2p core-level spectra (a) are taken from selected levels of the sputter depth profile (c) of PDMAAp/PEDOT, here indicated by arrows (level 1 = 30 s sputter time, level 35 = 1050 s sputter time, level 70 2100 s sputter time). The sputter depth profile of the pure hydrogel is depicted in (b). The profiles prove the homogeneous distribution of PEDOT (C—S group) within the hydrogel (C—SO_3— and N—C=O groups).

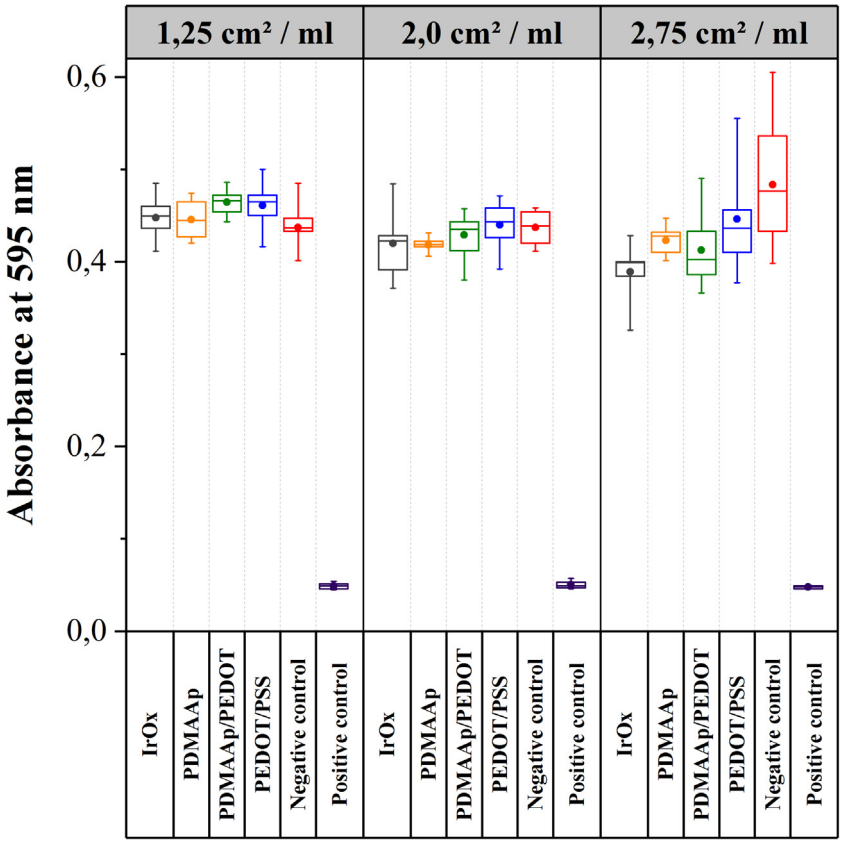

Fig. 8. In vitro elution toxicity study with the SH-SY5Y neuroblastoma cell-line. Box plots resent the absorbance at 595 nm measured at three different extract concentrations of the CPH and the control materials (n = 10 cell wells, except for the IrO_x and positive control at 2,75 cm^2/ml with n = 9).

this reason, extensive CV stressing over 1000 CV sweeps was used in this study to both evaluate the electrochemical and mechanical stability of the CPH system. We could thereby demonstrate that the CPH complex was electrochemically stable, with a reduction in CSC by only 1,9% over the 1000 CV sweeps tested. Interestingly, when observing the rate of change in the CSC of the unmodified PDMAAp hydrogel, we found a statistically significant increase by 36,4%. Since we could not observe any degradation of this material or change in the typical form of the CV over the 1000 cycles, we hypothesize that this increase in electroactivity results from rearrangements and infiltration of ions within the polymer. Stability is an essential quality of implants and the fact that the CPH can sustain substantial electrochemical stress without modification or degradation furthermore speak for that the PEDOT and the surface-attached PDMAAp hydrogel truly act as a hybrid unit.

Stable adhesion, the second design criterion in this work, was accomplished using 3-EBP silane. As described elsewhere, the 3-EBP silane introduces BP anchors, which are attached to the surface via silane. As a result of UV-irradiation, this BP moieties bind to C—H groups located in the backbone of the PDMAAp hydrogel matrix and form a covalent bond [29]. The successful functionalization of the IrO_x was here confirmed by a statistically significant increase in water contact angles showing that the attachment method is also applicable for IrO_x, a well-established electrode material for neural interfaces [34]. The strong adhesion expected to result from covalent attachment was demonstrated by that the CPH could endure the extensive CV cycling without substantially changing. Furthermore, we observed that the hydrogel could endure immersion during ultrasonication without any visually apparent delamination. In contrast, when coating an IrOx substrate without using the 3-EBP silane anchor, the hydrogel could be easily washed away. In summary we find that the CPH is adherent to the IrOx substrate even so additional adhesion tests will have to be performed in future work in order to quantify the bonding strength.

In addition to the extensive CV cycling in PBS, the electrochemical stability and long-term performance of the CPH was evaluated by immersing the CPH coated test samples in either PBS or cell culture medium for 10 days under physiological conditions. When comparing the CSCs after 0,5 h and 10 days for both in PBS and cell culture medium, we could obtain an increase by only of 5,7% and 3,0% respectively. It was interesting to see that the CPH material performs almost equally considering that the protein rich environment in the cell culture medium would challenge stable measurements over long time. In fact, we did not see major changes in stability upon immersion of the CPH samples in cell culture medium even after 52 days (data not shown), which is a good indicator for an expected non-biofouling effect of the hydrogel component. Pandiyarajan et al. have investigated the adsorption of blood proteins and cells on the PDMAA hydrogel and could demonstrate that this material is inert to blood proteins and platelet cells [35]. So far, the CPH however, has not specifically been tested with respect to protein adsorption. Further anti-biofouling characteristics of the CPH system will be analyzed in future studies together with specific applications.

The third design criterion was to develop a CPH which can be patterned onto selected electrode sites. Photolithographic micropatterning was demonstrated by UV- irradiation of the PDMAAp hydrogel through a foil mask, yielding different structures with smallest dimensions of 20 μm. Typical electrode sizes used for neural interfaces are 20–150 μm [30–32]. From this perspective, the proposed CPH presents a suitable candidate as

coating material. The patterning was demonstrated only for the hydrogel since the PEDOT is deposited into the already patterned hydrogel matrix. The final CPH is therefore microstructured as a consequence of PEDOT only being able to grow where the hydrogel is situated. The irregular edges, which can be seen in higher magnifications, are likely due to the limited precision of the foil mask. By establishing a fabrication and patterning process using photolithographic cleanroom technology together with chrome masks, we expect to accomplish more precise alignment and thus enable the coating of microfabricated electrodes with higher precision and dimensions as small as 5–10 μm.

Non-cytotoxicity of the CPH was demonstrated using an indirect elution test together with the neuroblastoma cell-line SH-SY5Y. Cell viability was calculated in percentage of the negative control and was higher than 85 % at all extract concentrations. No prominent loss of cell viability was observed when comparing the three different extract concentrations, speaking for that the material is non-cytotoxic. This conclusion was statistically verified using a two-way ANOVA model. The decreased viability, which was calculated at the highest extract concentration of 2,75 cm^2/ml, likely originates from a deviation of the negative control, which thus resulted in a higher reference representing 100 % viability. In addition, the ratio of test material exposed to cell culture medium was much larger than what is expected in a real implant scenario.

The individual components of the CPH have been studied for biomedical applications and there was, this far, no indication of any cytotoxicity or lack of biocompatibility of these materials [27,52–54]. We therefore have no reason to expect different results for a CPH being comprised of these building blocks. Scherag et al. have, for example, developed a coating system based on the benzophenone cross-linked PDMAA hydrogel to capture tumor cells in whole blood. In their study, they showed that fibroblasts could be successfully cultured in the presence of the hydrogel material [52]. The elution test here furthermore confirmed that components potentially leaking from the material had no cytotoxic effect.

To fully test the CPH as a coating material for implants, it is necessary to perform further biological analysis including direct cell contact tests and an evaluation of a potential cytotoxicity of benzophenone cross-linked polymers in complex biological environments. In this work, we focused on demonstrating the concept and design of the novel CPH, which offers patternability, surface attachment and a semi-interpenetrating network. The next step will thus be to perform further biological analysis and to test the material in the context of specific applications.

5. Conclusion

We report here on the formation of a novel hybrid material, a CPH, consisting of a hydrogel network containing PEDOT chains which shows excellent electrical properties. can be covalently attached to the substrate electrode and can be photolithographically micropatterned onto selected electrode sites. Homogeneous integration of PEDOT into the hydrogel matrix was confirmed with CV, EIS and XPS measurements. Non-cytotoxicity was verified using a cell elution test together with a neuroblastoma cell-line proving biological relevance of the formed material. The CPH presented in this work thereby addresses the challenge of forming a stable and adherent coating system and shows great potential for a wide range of future applications.

Acknowledgements

This work was supported by BrainLinks-BrainTools, Cluster of Excellence funded by the German Research Foundation (DFG, Grant number EXC 1086). The K-Alpha+ instrument was financially supported by the Federal Ministry of Economics and Technology on the basis of a decision by the German Bundestag. Furthermore, we would like to thank A. Schopf for supporting the cell culture experiments, M. Kurowska for fabricating the 3-EBP silane and N. Birsner, C. Boehler and D. Plachta for helpful advice and discussions.

Appendix A. Supplementary data

Supplementary data associated with this article can be found, in the online version, at http://dx.doi.org/10.1016/j.actbio.2017.05.056.

References

[1] B.S. Wilson, M.F. Dorman, Cochlear implants: a remarkable past and a brilliant future, Hearing Res. 242 (2008) 3–21.
[2] D. Guiraud, T. Stieglitz, K.P. Koch, J.L. Divoux, P. Rabischong, An implantable neuroprosthesis for standing and walking in paraplegia: 5-year patient follow-up, J. Neural Eng. 3 (2006) 268–275.
[3] A.L. Benabid, S. Chabardes, J. Mitrofanis, P. Pollak, Deep brain stimulation of the subthalamic nucleus for the treatment of Parkinson's disease, Lancet Neurol. 8 (2009) 67–81.
[4] J.P. Rauschecker, R.V. Shannon, Sending sound to the brain, Science 295 (2002) 1025–1029.
[5] M. Jorfi, J.L. Skousen, C. Weder, J.R. Capadona, Progress towards biocompatible intracortical microelectrodes for neural interfacing applications, J. Neural Eng. 12 (2015) 011001.
[6] R. Biran, D.C. Martin, P.A. Tresco, Neuronal cell loss accompanies the brain tissue response to chronically implanted silicon microelectrode arrays, Exp. Neurol. 195 (2005) 115–126.
[7] V.S. Polikov, P.A. Tresco, W.M. Reichert, Response of brain tissue to chronically implanted neural electrodes, J. Neurosci. Methods 148 (2005) 1–18.
[8] R.A. Green, S. Baek, L.A. Poole-Warren, P.J. Martens, Conducting polymer-hydrogels for medical electrode applications, Sci. Technol. Adv. Mater. 11 (2010).
[9] A. Guiseppi-Elie, Electroconductive hydrogels: synthesis, characterization and biomedical applications, Biomaterials 31 (2010) 2701–2716.
[10] M. Asplund, T. Nyberg, O. Inganas, Electroactive polymers for neural interfaces, Polym. Chem.-UK 1 (2010) 1374–1391.
[11] K. Gilmore, A.J. Hodgson, B. Luan, C.J. Small, G.G. Wallace, Preparation of hydrogel conducting polymer composites, Polym. Gels Netw. 2 (1994) 135–143.
[12] M. Asplund, C. Boehler, T. Stieglitz, Anti-inflammatory polymer electrodes for glial scar treatment: bringing the conceptual idea to future results, Front. Neuroeng. 7 (2014) 9.
[13] C. Boehler, C. Kleber, N. Martini, Y. Xie, I. Dryg, T. Stieglitz, U.G. Hofmann, M. Asplund, Actively controlled release of Dexamethasone from neural microelectrodes in a chronic in vivo study, Biomaterials 129 (2017) 176–187.
[14] T. Nyberg, O. Inganas, H. Jerregard, Polymer hydrogel microelectrodes for neural communication, Biomed. Microdevices 4 (2002) 43–52.
[15] D.H. Kim, M. Abidian, D.C. Martin, Conducting polymers grown in hydrogel scaffolds coated on neural prosthetic devices, J. Biomed. Mater. Res. A 71 (2004) 577–585.
[16] R.A. Green, R.T. Hassarati, J.A. Goding, S. Baek, N.H. Lovell, P.J. Martens, L.A. Poole-Warren, Conductive hydrogels: mechanically robust hybrids for use as biomaterials, Macromol. Biosci. 12 (2012) 494–501.
[17] S. Brahim, D. Narinesingh, A. Guiseppi-Elie, Polypyrrole-hydrogel composites for the construction of clinically important biosensors, Biosens. Bioelectron. 17 (2002) 53–59.
[18] C.J. Small, C.O. Too, G.G. Wallace, Responsive conducting polymer-hydrogel composites, Polym. Gels Netw. 5 (1997) 251–265.
[19] L.M. Lira, S.I.C. de Torresi, Conducting polymer-hydrogel composites for electrochemical release devices: synthesis and characterization of semi-interpenetrating polyaniline-polyacrylamide networks, Electrochem. Commun. 7 (2005) 717–723.
[20] N. Paradee, A. Sirivat, Electrically controlled release of benzoic acid from poly (3,4-ethylenedioxythiophene)/alginate matrix: effect of conductive poly(3,4-ethylenedioxythiophene) morphology, J. Phys. Chem. B 118 (2014) 9263–9271.
[21] M.R. Abidian, E.D. Daneshvar, B.M. Egeland, D.R. Kipke, P.S. Cederna, M.G. Urbanchek, Hybrid conducting polymer-hydrogel conduits for axonal growth and neural tissue engineering, Adv. Healthc. Mater. 1 (2012) 762–767.
[22] M.B. Runge, M. Dadsetan, J. Baltrusaitis, T. Ruesink, L.C. Lu, A.J. Windebank, M.J. Yaszemski, Development of electrically conductive oligo(polyethylene glycol) fumarate-polypyrrole hydrogels for nerve regeneration, Biomacromolecules 11 (2010) 2845–2853.
[23] L. Pan, G. Yu, D. Zhai, H.R. Lee, W. Zhao, N. Liu, H. Wang, B.C. Tee, Y. Shi, Y. Cui, Z. Bao, Hierarchical nanostructured conducting polymer hydrogel with high electrochemical activity, Proc. Natl. Acad. Sci. U.S.A. 109 (2012) 9287–9292.

[24] G.L.M. Cheong, K.S. Lim, A. Jakubowicz, P.J. Martens, L.A. Poole-Warren, R.A. Green, Conductive hydrogels with tailored bioactivity for implantable electrode coatings, Acta Biomater. 10 (2014) 1216–1226.
[25] D.H. Kim, J.A. Wiler, D.J. Anderson, D.R. Kipke, D.C. Martin, Conducting polymers on hydrogel-coated neural electrode provide sensitive neural recordings in auditory cortex, Acta Biomater. 6 (2010) 57–62.
[26] L. Rao, H.H. Zhou, T. Li, C.Y. Li, Y.W.Y. Duan, Polyethylene glycol-containing polyurethane hydrogel coatings for improving the biocompatibility of neural electrodes, Acta Biomater. 8 (2012) 2233–2242.
[27] C. Hadler, P. Aliuos, G. Brandes, A. Warnecke, J. Bohlmann, W. Dempwolf, H. Menzel, T. Lenarz, G. Reuter, K. Wissel, Polymer coatings of cochlear implant electrode surface – an option for improving electrode-nerve-interface by blocking fibroblast overgrowth, PLoS One 11 (2016) e0157710.
[28] G. Justin, A. Guiseppi-Elie, Electroconductive blends of poly(HEMA-co-PEGMA-co-HMMA-co-SPMA) and poly(Py-co-PyBA). In vitro biocompatibility, J Bioact. Compat. Polym. 25 (2010) 121–140.
[29] O. Prucker, C.A. Naumann, J. Ruhe, W. Knoll, C.W. Frank, Photochemical attachment of polymer films to solid surfaces via monolayers of benzophenone derivatives, J. Am. Chem. Soc. 121 (1999) 8766–8770.
[30] T. Boretius, K. Yoshida, J. Badia, K. Harreby, A. Kundu, X. Navarro, W. Jensen, T. Stieglitz, A transverse intrafascicular multichannel electrode (TIME) to treat phantom limb pain – towards human clinical trials, in: P Ieee Ras-Embs Int, 2012, pp. 282-287.
[31] T. Stieglitz, T. Boretius, J. Ordonez, C. Hassler, C. Henle, W. Meier, D.T.T. Plachta, M. Schuettler, Miniaturized neural interfaces and implants, in: Proc Spie, 2012;8251.
[32] S. Herwik, S. Kisban, A.A.A. Aarts, K. Seidl, G. Girardeau, K. Benchenane, M.B. Zugaro, S.I. Wiener, O. Paul, H.P. Neves, P. Ruther, Fabrication technology for silicon-based microprobe arrays used in acute and sub-chronic neural recording, J. Micromech. Microeng. 19 (2009).
[33] S. Loschonsky, K. Shroff, A. Worz, O. Prucker, J. Ruhe, M. Biesalski, Surface-attached PDMAA-GRGDSP hybrid polymer monolayers that promote the adhesion of living cells, Biomacromolecules 9 (2008) 543–552.
[34] P. Aliuos, A. Sen, U. Reich, W. Dempwolf, A. Warnecke, C. Hadler, T. Lenarz, H. Menzel, G. Reuter, Inhibition of fibroblast adhesion by covalently immobilized protein repellent polymer coatings studied by single cell force spectroscopy, J. Biomed. Mater. Res. A 102 (2014) 117–127.
[35] C.K. Pandiyarajan, O. Prucker, B. Zieger, J. Ruhe, Influence of the molecular structure of surface-attached poly(N-alkyl acrylamide) coatings on the interaction of surfaces with proteins, cells and blood platelets, Macromol. Biosci. 13 (2013) 873–884.
[36] A. Worz, B. Berchtold, K. Moosmann, O. Prucker, J. Ruhe, Protein-resistant polymer surfaces, J. Mater. Chem. 22 (2012) 19547–19561.
[37] M. Tallawi, E. Rosellini, N. Barbani, M.G. Cascone, R. Rai, G. Saint-Pierre, A.R. Boccaccini, Strategies for the chemical and biological functionalization of scaffolds for cardiac tissue engineering: a review, J. R. Soc. Interface 12 (2015).
[38] X.H. Liu, P.X. Ma, Polymeric scaffolds for bone tissue engineering, Ann. Biomed. Eng. 32 (2004) 477–486.
[39] H. Yamato, M. Ohwa, W. Wernet, Stability of polypyrrole and poly(3,4-ethylenedioxythiophene) for biosensor application, J. Electroanal. Chem. 397 (1995) 163–170.
[40] M. Gianneli, R.F. Roskamp, U. Jonas, B. Loppinet, G. Fytas, W. Knoll, Dynamics of swollen gel layers anchored to solid surfaces, Soft Matter 4 (2008) 1443–1447.
[41] R. Toomey, D. Freidank, J. Ruhe, Swelling behavior of thin, surface-attached polymer networks, Macromolecules 37 (2004) 882–887.
[42] K.L. Parry, A.G. Shard, R.D. Short, R.G. White, J.D. Whittle, A. Wright, ARXPS characterisation of plasma polymerised surface chemical gradients, Surf. Interface Anal. 38 (2006) 1497–1504.
[43] J.H. Scofield, Hartree-Slater subshell photoionization cross-sections at 1254 and 1487 ev, J. Electron Spectrosc. 8 (1976) 129–137.
[44] S. Tanuma, C.J. Powell, D.R. Penn, Calculations of electron inelastic mean free paths. 5. Data for 14 organic-compounds over the 50–2000 ev range, Surf. Interface Anal. 21 (1994) 165–176.
[45] T. Mosmann, Rapid colorimetric assay for cellular growth and survival – application to proliferation and cyto-toxicity assays, J. Immunol. Methods 65 (1983) 55–63.
[46] P. Zou, W. Hartleb, K. Lienkamp, It takes walls and knights to defend a castle – synthesis of surface coatings from antimicrobial and antibiofouling polymers, J. Mater. Chem. 22 (2012) 19579–19589.
[47] O. Bubnova, Z.U. Khan, A. Malti, S. Braun, M. Fahlman, M. Berggren, X. Crispin, Optimization of the thermoelectric figure of merit in the conducting polymer poly(3,4-ethylenedioxythiophene), Nat. Mater. 10 (2011) 429–433.
[48] A.A. Farah, S.A. Rutledge, A. Schaarschmidt, R. Lai, J.P. Freedman, A.S. Helmy, Conductivity enhancement of poly(3,4-ethylenedioxythiophene)-poly (styrenesulfonate) films post-spincasting, J. Appl. Phys. 112 (2012).
[49] M. Bruns, C. Barth, P. Bruner, S. Engin, T. Grehl, C. Howell, P. Koelsch, P. Mack, P. Nagel, V. Trouillet, D. Wedlich, R.G. White, Structure and chemical composition of mixed benzylguanine- and methoxy-terminated self-assembled monolayers for immobilization of biomolecules, Surf. Interface Anal. 44 (2012) 909–913.
[50] J. Goding, A. Gilmour, P. Martens, L. Poole-Warren, R. Green, Interpenetrating conducting hydrogel materials for neural interfacing electrodes, Adv. Healthc. Mater. (2017).
[51] C. Boehler, F. Oberueber, S. Schlabach, T. Stieglitz, M. Asplund, Long-term stable adhesion for conducting polymers in biomedical applications: IrOx and nanostructured platinum solve the chronic challenge, ACS Appl. Mater. Interfaces 9 (2017) 189–197.
[52] F.D. Scherag, R. Niestroj-Pahl, S. Krusekopf, K. Lucke, T. Brandstetter, J. Ruhe, Highly selective capture surfaces on medical wires for fishing tumor cells in whole blood, Anal. Chem. 89 (2017) 1846–1854.
[53] R.M. Miriani, M.R. Abidian, D.R. Kipke, Cytotoxic analysis of the conducting polymer PEDOT using myocytes, IEEE Eng. Med. Biol. (2008) 1841–1844.
[54] M. Asplund, E. Thaning, J. Lundberg, A.C. Sandberg-Nordqvist, B. Kostyszyn, O. Inganas, H. von Holst, Toxicity evaluation of PEDOT/biomolecular composites intended for neural communication electrodes, Biomed. Mater. 4 (2009) 045009.